



### **Science Arts & Métiers (SAM)**

is an open access repository that collects the work of Arts et Métiers Institute of Technology researchers and makes it freely available over the web where possible.

This is an author-deposited version published in: <https://sam.ensam.eu>  
Handle ID: <http://hdl.handle.net/10985/26090>

#### **To cite this version :**

Qin HAO, Zouhair MALHI, Pierre-Marc FRANÇOIS, Emmanuel RICHAUD - Hyperelasticity modelling for thermally aged silicones - Polymer Bulletin - Vol. 81, n°2, p.1249-1268 - 2024

Any correspondence concerning this service should be sent to the repository

Administrator : [scienceouverte@ensam.eu](mailto:scienceouverte@ensam.eu)



# 1 HYPERELASTICITY MODELING FOR THERMALLY AGED SILICONES

2 Qin Hao<sup>1</sup>, Zouhair Malhi<sup>2</sup>, Pierre Marc François<sup>2</sup>, Emmanuel Richaud<sup>1\*</sup>

3

4 1. PIMM, Arts et Metiers Institute of Technology, CNRS, Cnam, HESAM University, 151  
5 boulevard de l'Hopital, 75013 Paris (France)

6 2. BONE 3D, 14 Rue Jean Antoine de Baïf, 75013 Paris (France).

7

8 \* corresponding author : emmanuel.richaud@ensam.eu

9

## 10 ABSTRACT

11 Two families of Room Temperature Vulcanized PDMS **with different hardness** were thermally  
12 aged. Mechanical properties were monitored by tensile tests and macromolecular architecture  
13 was followed by differential scanning calorimetry (crystallization) and sol gel analysis  
14 (swelling degree). Data showed that PDMS display a loss of plasticity due to a crosslinking  
15 process. The main novelty was to describe mechanical behavior by a **hyperelastic so called**  
16 **Ogden's model** whose coefficients were correlated with macromolecular properties and then  
17 ageing degree. The model coefficients were also used to derive an embrittlement criterion.

18

## 19 KEYWORDS

20 Silicone Rubber, thermal ageing, mechanical properties, crosslinking

21

## 22 1. INTRODUCTION

23

24 Room temperature vulcanization (RTV) **silicone rubbers** are commonly used in the biomedical  
25 field. **They are obtained by blending vinyl terminated PDMS linear polymers with a PDMS**  
26 **containing some hydrosilane groups. The reaction between hydrosilane and vinyl is catalyzed**  
27 **by organoplatinum molecules and forms an insoluble network.**

28 The thermal stability of PDMS has been extensively studied in the literature. **TGA studies were**  
29 **performed under nitrogen or oxygen atmosphere. Thanks to the coupling of TGA with analysis**  
30 **of volatiles compounds, the degradation mechanisms were better understood [1,2]. Under inert**  
31 **atmosphere, an “unzipping” mechanism possibly by concerted rearrangement occurring in**  
32 **random position of the PDMS chains was proposed.** Under air, the same kinds of volatiles  
33 species are observed [1], but the presence of oxygen seems to induce some increase in crosslink  
34 density The effect of aromatic comonomers [3], or fillers was also illustrated [4,5].

35 **Only a few papers deal with isothermal degradation. Lacoste and coll [6] investigated the**  
36 **thermal degradation of PDMS based copolymers, in which a significant oxidation was observed**

1

1

2

37 possibly due to the aliphatic nature of comonomers. Other illustrate the modeling of joint radio  
38 thermal aging [7]. It seems clear that ageing under air induces a crosslinking mechanism leading  
39 to increase in elastic moduli, and decrease in ultimate strain [8]. The effect of chemical changes  
40 on mechanical properties constitutes the missing link in predicting the lifetime of thermally  
41 aged PDMS. A recent paper [9] illustrated the link between mass loss and elastic modulus  
42 increase but this remains to be generalized. In particular, the identification of the critical state  
43 corresponding to the loss of mechanical properties and/or the existence of a causal chain  
44 allowing the embrittlement to be predicted remains an open question.

45 To answer to those questions, this paper aims at:

46 - Perform thermal ageing at various temperatures on PDMS differing by their initial crosslink  
47 densities, commonly described by their hardness.

48 - Perform a multiscale monitoring of ageing so as to identify the nature of macromolecular  
49 change.

50 - Propose the relationship between structure to link macromolecular changes and drop of  
51 mechanical properties.

52

## 53 2. EXPERIMENTAL

54

### 55 2.1. Samples Preparation

56 RTV silicones obtained by mixing part A (“base”) and part B (“catalyst”) i.e. PDMS chains  
57 functionalized by hydrosilane and PDMS functionalized by vinylenes. Pt catalyst is present in  
58 only one of the parts so that reaction starts when part A and part B are mixed. Samples were  
59 manufactured in 2 mm thick samples according to ISO 527-2 5B standard by injecting parts A  
60 and B into acrylic 3D printed molds. Two PDMS grades differing by their hardnesses (15A and  
61 30A) are investigated here. Some details are given in Supplementary Information. Dogbones  
62 samples were aged and analyzed by mechanical testing. Some other were used for DSC,  
63 gravimetry and sol gel analysis.

64 The heterogeneity due to diffusion-limited oxidation will not be considered in the following.  
65 One thing to note is that the oxygen diffusivity in PDMS is almost 10 to 100 times higher than  
66 any other rubber [10] meanwhile those rubbers degrade quite slowly compared to other polymers  
67 [11]. The original densities of both materials were measured to be 1.100 for PDMS 15A and  
68 1.113 for PDMS 30A.

69

### 70 2.2. Ageing procedures

71 Samples were isothermally aged under air at various temperatures (180, 200, 220 and 250°C)  
72 in ventilated ovens (AP60, System Climatic France). Isothermal ageing durations ranged from  
73 4h-30h (for ageing at 250°C) to about 1 year (for ageing at 180°C).

74

## 75 2.3. Characterization methods

76

### 77 2.2.1. Tensile tests

78 Samples were made in dog bone shape according to ISO 527-2 – 5B. The testings were  
79 performed by Instron 4301 tensile machine with a 100 N load cell. The testing speed was set at  
80 10 mm.min<sup>-1</sup> elongation rate. 3 samples were tested per condition.

81

### 82 2.2.2. Sol gel analysis

83 Samples ( $m_0$  about 100 mg) were immersed in toluene. After 72 h, the swollen mass  $m_{swollen}$  was  
84 estimated. NB: this duration was verified to correspond to the equilibrium for solvent ingress.  
85 Samples were thus left and the mass of dried samples  $m_{dried}$  corresponding to the insoluble  
86 network was measured after 24h drying. Data were used to estimate:

87 The swelling ratio:

88 
$$SR = \frac{m_{swollen} - m_{dried}}{m_{swollen}} (1)$$

89 The soluble fraction:

90 
$$SF = \frac{m_0 - m_{dried}}{m_0} (2)$$

91

### 92 2.2.3. Differential Scanning Calorimetry

93 Approximately 10 mg of sample was analyzed using a Q1000 DSC device (TA Instruments).  
94 The samples were placed in sealed aluminum pans, cooled from room temperature to -85°C, and  
95 then heated to -40°C. DSC cell was continuously purged by a nitrogen flow of 50 ml min<sup>-1</sup>. Data  
96 were processed using TA Analysis software. The DSC was calibrated with an indium standard  
97 before the experiment.

98

### 99 2.2.4. Gravimetry

100 Samples (initial mass 0.5 – 1 g) were regularly weighted after ageing using an AT261  
101 DeltaRange balance (Mettler Toledo) with an accuracy higher than 0.1 mg meaning that the  
102 uncertainty is lower than 0.01%.

103

### 104 2.2.5. Thermogravimetric analysis

105 TGA measurements were performed using a Q500 apparatus driven by QSeries Explorer (TA  
106 Instruments). Isothermal measurements were performed under 100% N<sub>2</sub> atmosphere supplied  
107 by a continuous 50 ml min<sup>-1</sup> gas flow. Isothermal degradation was performed at a constant

5

3

6

108 temperature equal to 500°C. Papers dealing with anisothermal degradation monitored by TGA  
109 under nitrogen [1,2] suggest that (i) onset of mass loss curves is close to 500°C and (ii) cyclic  
110 oligomers are released, in line with an unzipping mechanism. This is the reason why this  
111 temperature was chosen. It is possible that the same mechanism occurs at lower temperature, but  
112 in a timescale unsuitable with simple lab tests.

113

### 114 3. RESULTS

115

#### 116 3.1. Changes of mechanical properties during thermal ageing

117

118 **Figure 1** displays stress-strain curves for virgin and degraded PDMS after ageing at 180°C  
119 under air (**Figures 1a and 1c**) and after ageing at 250°C (**Figures 1b and 1d**). At first, it is clear  
120 that ageing induced the same kind of consequences either for PDMS 15A and for PDMS 30A.  
121 Identically to literature [12, 13, 14, 15, 16], curves for unaged polymers display a hyperelastic behavior  
122 with two domains: one corresponding to low strains (typically < 200 %) and another associated  
123 to high strains (typically > 500%). The possibility of Stress Induced Crystallization was rejected  
124 for two reasons: first, according to previous papers, this phenomenon occurs at very low  
125 temperature [17], and secondly, SIC is expected to disappear in the case where ageing induces  
126 crosslinking [18] (which is the case here, as it will be seen later). Basing on a previous work by  
127 Mark and Coll [19], the « low strain domain » would correspond to the presence of long  
128 elastically active chains whereas the « high strain domain », would express the presence of  
129 shorter chains. In the « intermediate » domain, we guess that mechanical behaviour for instance  
130 at 300% is the same than at 100 or 200% since elastic modulus values are very close and linked to  
131 the stretching of long chains.

132

133

134

135

136

137

138

139

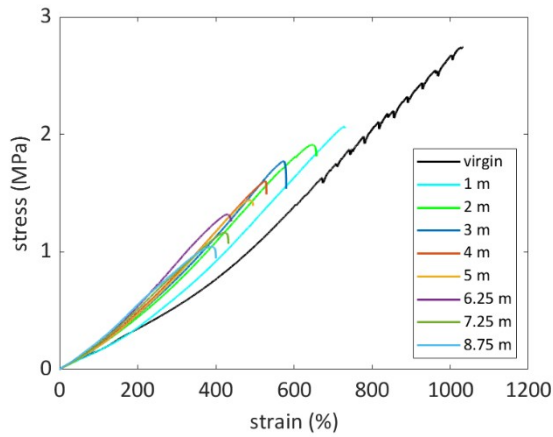
140

141

142

143

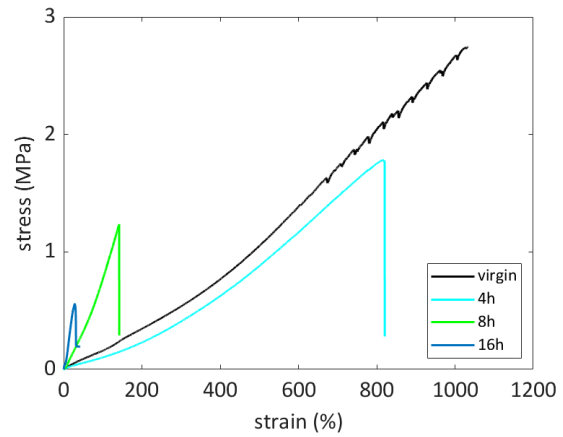
144



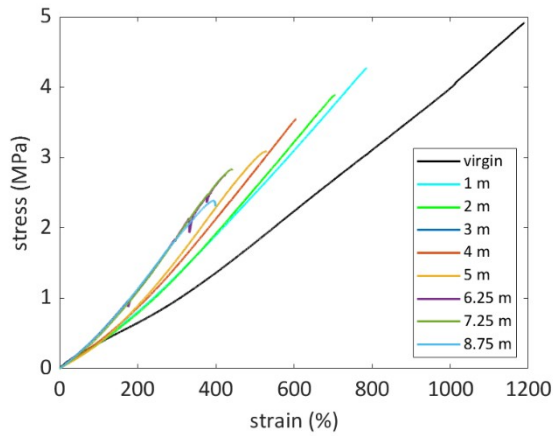
145

146

(a)



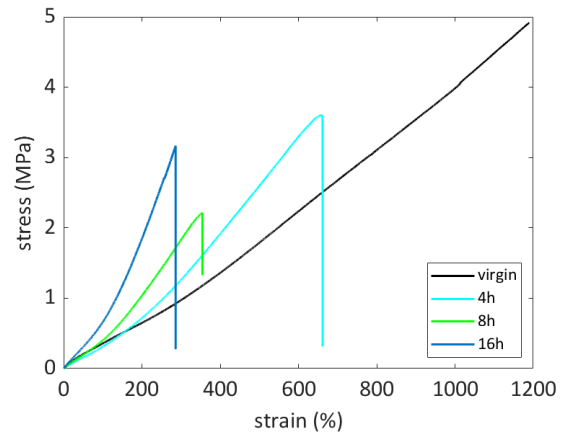
(b)



147

148

(c)



(d)

149 **Figure 1. Stress strain curves of PDMS RTV 15A (a, b) and 30A (c, d) aged at 180°C (a,**  
150 **c) and 250°C (c, d) under air. NB: ageing durations are given in months.**

151

152 After thermal ageing, it is mainly observed that:

153 - ultimate elongation decreases but stays higher than 400% after almost 9 months at 180°C.

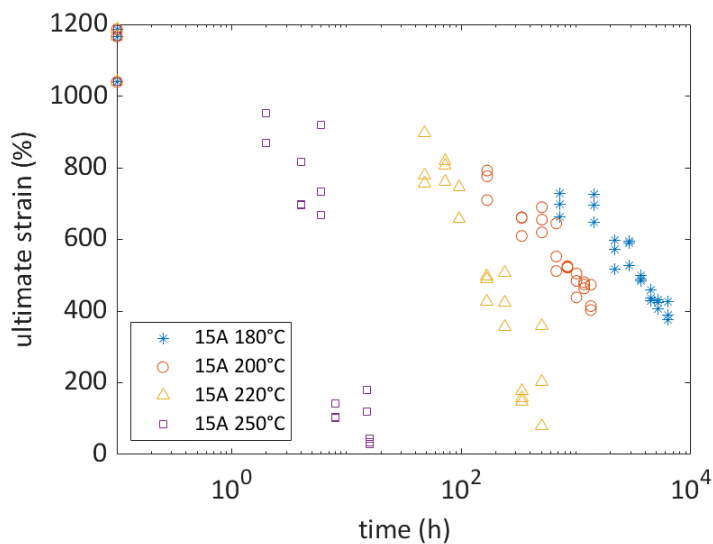
154 - the domain expressing the « shortest » chain seems to predominate over the domain  
155 corresponding to the long chains, which seems to indicate the conversion of « long » elastically  
156 active chains into « short » ones, i.e. a crosslinking mechanism. **This will be confirmed by the**  
157 **modeling of stress strain curves using an hyperelastic model as explained in the “discussion**  
158 **section”.**

159 **Those observations seem valid in the whole range of temperatures under investigation (Figures**  
160 **1a vs 1b and 1c vs 1d).**

161

162 Ageing at other temperatures ranging from 180°C to 250°C were also performed. Changes of  
163 ultimate strain and stress are given in **Figures 2** and **3**. Overall, the characteristic degradation  
164 times are relatively close for both rubbers, which will be commented in the “discussion” section.

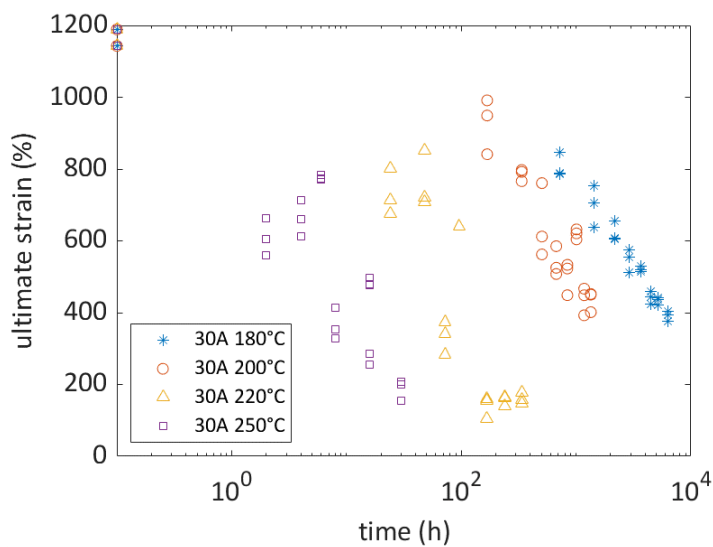
165



166

167

(a)



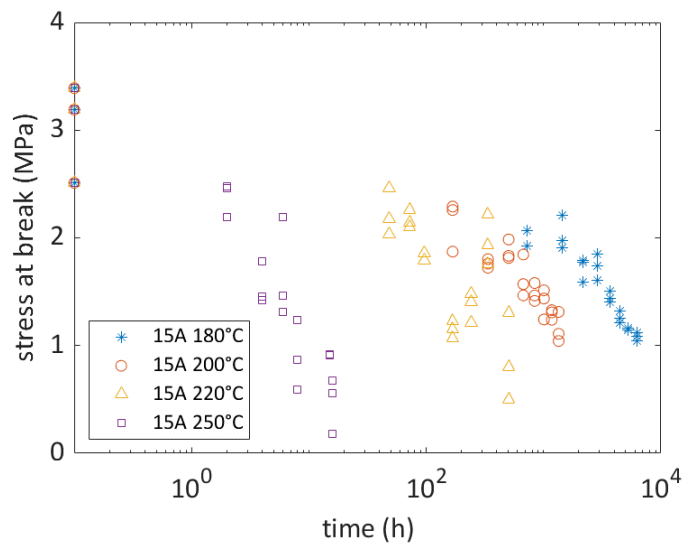
168

169

(b)

170 **Figure 2. Changes of ultimate strain for PDMS 15A (a) and 30A (b) for thermal ageing**  
171 **under air.**

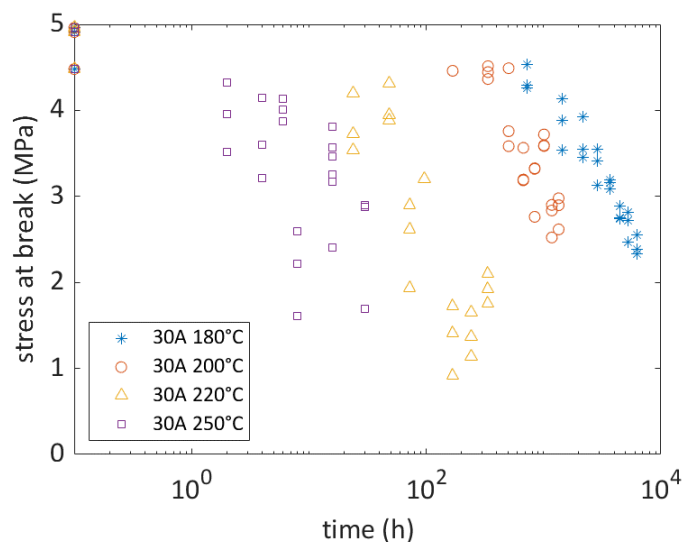
172



173

174

(a)



175

176

(b)

177 **Figure 3. Changes of stress at break for PDMS 15A (a) and 30A (b) for thermal ageing**  
 178 **under air.**

179

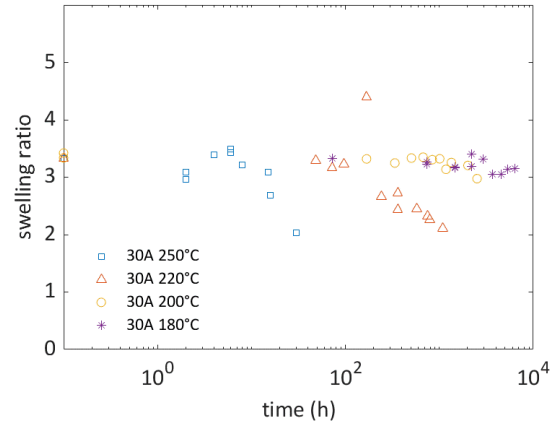
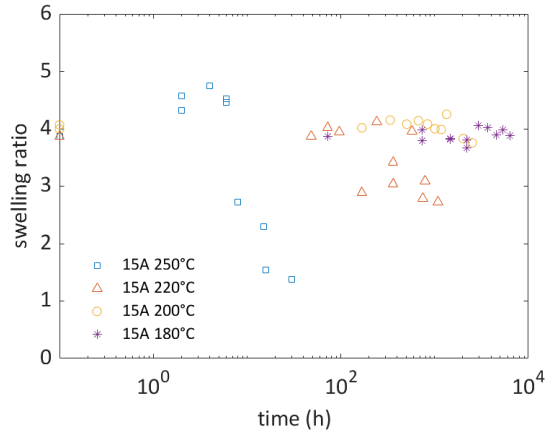
### 180 3.2. Macromolecular changes

181

182 The effect of ageing on macromolecular architecture was first investigated by sol gel analysis.  
 183 Toluene absorption is used here as a probe to estimate the crosslink density, which is expected to  
 184 change with thermal aging due to oxidation-induced crosslinking and/or chain scission. The  
 185 changes in swelling ratio and soluble fraction are shown in **Figure 4**.

186

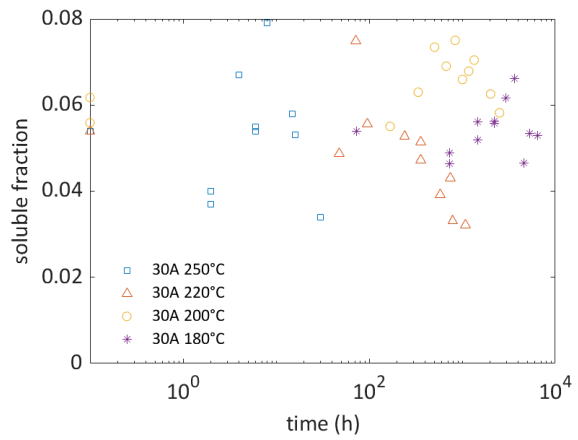
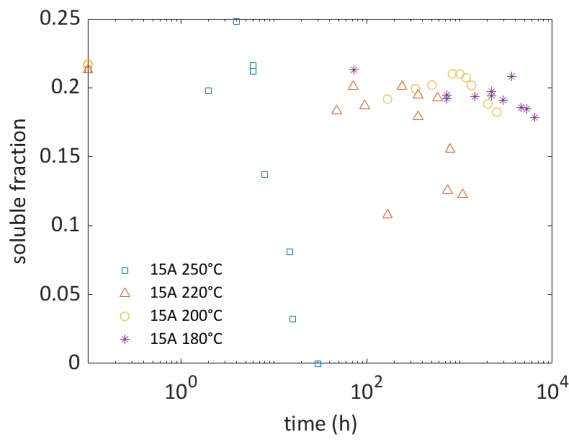




187

188

(a)



189

190

(b)

**Figure 4. Changes of swelling ratio (a) and soluble fraction (b).**

191

192

193 The concentration in elastically active chains  $n_A$  can be calculated from the Flory  
194 Rehner equation [20]:

195

196

$$-\left[\ln(1-\phi) + \phi + \chi \cdot \phi^2\right] = V_{m\text{toluene}} \cdot n_A \cdot \left(\phi^{\frac{1}{3}} - \frac{2\phi}{f}\right) \quad (3)$$

197

198 In which:

199 -  $n_A$  is the concentration in elastically active chains ( $\text{mol l}^{-1}$ ).

200 -  $\phi$  is the volume fraction of PDMS in the PDMS-toluene swollen mixture

201 -  $V_{m\text{toluene}}$  is the toluene molar volume ( $106.1 \text{ cm}^3 \text{ mol}^{-1}$ ).

202 -  $f$  is the functionality of PDMS network

203 -  $\chi$  is the Flory parameter describing the interaction between PDMS and toluene.

204

205 Using  $f = 3$ ,  $\chi \sim 0.54$ ,  $n_A$  values coming from **Eq. 3** can be found in good agreement with values  
 206 coming from the classical rubber elasticity equation used here for the data obtained in the low  
 207 deformation domain of **Figure 1**, typically at strains lower than 50% i.e.  $\lambda < 1.5$  [21]:

$$208 \quad \sigma_0 = n_A RT \cdot \left( \lambda - \frac{1}{\lambda^2} \right) \quad (4)$$

209

210 where  $\sigma_0$  is the nominal stress and  $\lambda$  is the draw ratio. Results are given in **Table 1**. It must be  
 211 emphasized that  $\chi$  was adjusted. Its value is found slightly higher than in literature, where there  
 212 is certain discrepancy about  $\chi$  values for the PDMS-toluene mixture in literature. For example,  
 213 its value is given by  $\chi = 0.459 + 0.134\phi + 0.59\phi^2$  [22] or  $\chi = 0.452 + 0.265\phi$  [23].

214

	SR	SF	$\phi_P$	$\chi$	$n_A$ (Eq. 3)	$n_A$ (Eq. 4)	$\chi$ [22]	$\chi$ [23]
15A	3.873	0.213	0.215	0.54	42.4	42.8	0.52	0.51
30A	3.329	0.054	0.250	0.54	81.6	79.1	0.53	0.52

215 **Table 1. Sol gel properties of PDMS where SR is the swelling ratio, SF the soluble**  
 216 **fraction,  $\phi_P$  is the volume fraction of polymer in the swollen network,  $n_A$  is adjusted from**  
 217 **Eq. 3 and from Eq. 4 and comparison with  $\chi$  values from literature.**

218

219 In the following, to avoid the uncertainties linked to the  $\chi$  value in aged network, the “raw” sol  
 220 gel properties data will be discussed instead of their exploitation using Eq. 3. Despite the  
 221 uncertainties due to sol gel measurements, at 250°C, a significant decrease seems to be observed  
 222 in both swollen ratio and soluble fraction, which is evidence of a predominant crosslinking. The  
 223 same occurs at lower temperature but in a lower extent. Interestingly, mechanical properties  
 224 seem to drop meanwhile sol gel properties are hardly changed. This will be discussed in the  
 225 following in terms of structure properties involved for predicting embrittlement.

226

227 The crystallization and melting of PDMS were also investigated by DSC (**Figure 5**). For unaged  
 228 PDMS 15A and 30A samples, a crystallization peak is observed at -70°C, and is accompanied  
 229 by a melting peak at about -45°C, consistently with literature [24]. Values for crystallization are  
 230 given in Table 2. More in detail:

231 - Unaged PDMS 15A sample displays a higher crystallization temperature than PDMS 30A on  
 232 both peak onset and the maximal temperature.

233 - The crystallization peak of PDMS 15A is obviously broader than PDMS 30A. A tentative  
 234 explanation for the broadness of crystallization peak is due to the heterogeneity (bimodality) of  
 235 crosslinking network. This will be confirmed by the value of constants expressing  
 236 hyperelasticity, namely  $c_{\alpha=3}$ ,  $c_{\alpha=2}$ , determined in the ‘Discussion’ section.

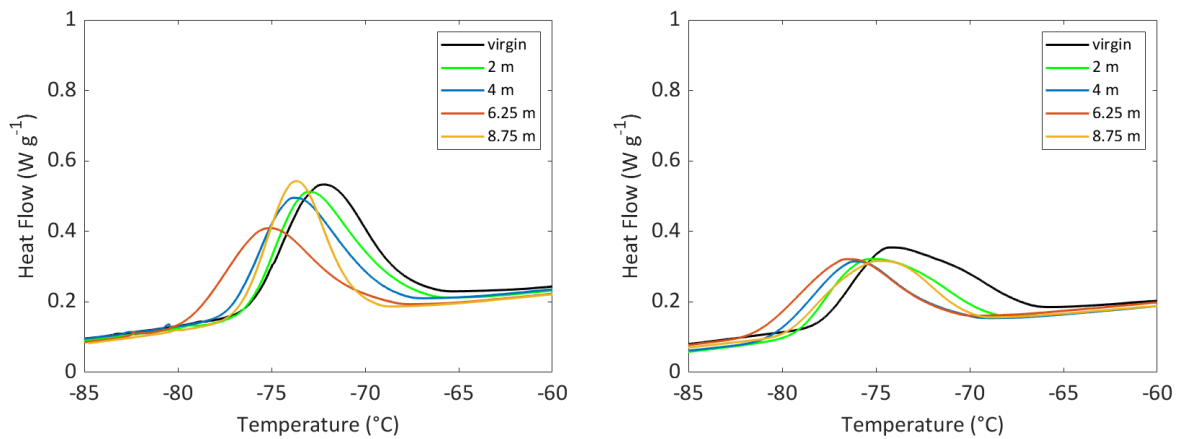
237 - During ageing, all the samples display a decrease of the crystallization temperature, together  
 238 with the onset and the crystallization enthalpy which will be discussed later. Those observations  
 239 are consistent with other polymers undergoing ageing induced crosslinking, since increase in  
 240 molar mass implies reduced of macromolecular mobility [25].

241

	$T_c$ (°C)	$T_{onset}$ (°C)	$\Delta H_c$ (J g <sup>-1</sup> )
<b>PDMS 15A</b>	-72.3	-67.6	17.6
<b>PDMS 30A</b>	-74.3	-66.8	13.3

242

Table 2. Parameters of crystallization for unaged PDMS.

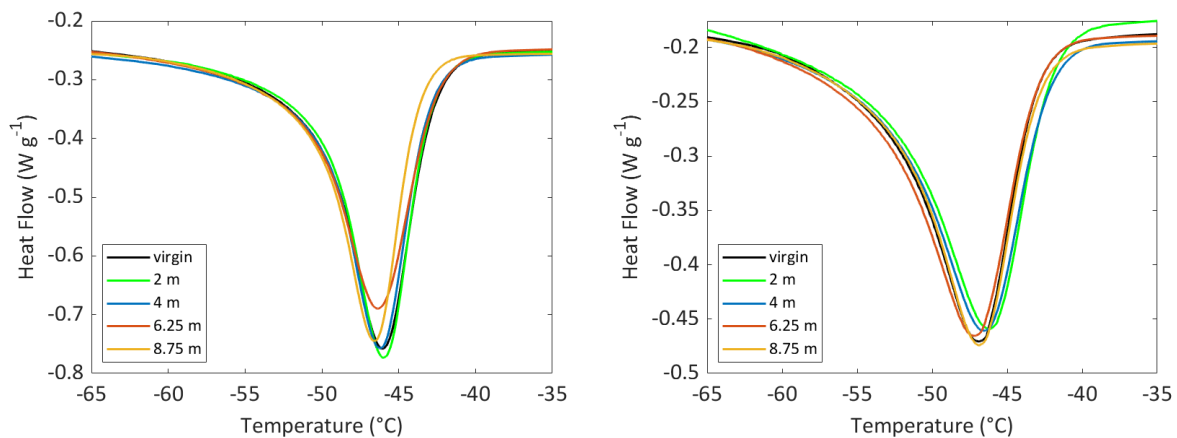


243

244

(a)

(b)



245

246

(c)

(d)

247 **Figure 5. DSC thermograms of PDMS for crystallization (a, b) and melting (c, d) for**  
 248 **PDMS 15A (a, c) and 30 A (b, d).**

249

250 Dealing now with melting, a very slight decrease is observed in melting temperature. It is for  
 251 example consistent with observation by Labouriau et al [17] where crystallization temperature  
 252 decreases faster than melting temperature for gamma irradiated PDMS. The latter can be

253 commented as follows: according to Flory, the melting temperature  $T_m$  of a copolymer is  
254 depressed compared to the value of homopolymer  $T_{m0}$ , as described by the general formula [26]:

255 
$$\frac{1}{T_m} - \frac{1}{T_{m0}} = \frac{-R}{\Delta H_m} \ln(p) - \frac{R}{\Delta H_m} x_B \quad (5)$$

256

257  $\Delta H_m$  being the melting enthalpy of crystallizable unit, p the probability of finding an  
258 homopolymer **crystallizable** sequence and  $x_B$  the fraction of non-crystallizable defect B  
259 (**comonomers in the Flory's paper, crosslink sites in this work**).

260 Here, the depletion of melting temperature is consistent with the existence of a crosslinking,  
261 under the assumption that crosslinking nodes behave as molecular defects inhibiting the  
262 crystallization.

263

264 Last, residual mass was monitored for thermally aged samples. Two kinds of experiments were  
265 conducted:

266 - measurement of mass loss for thermal oxidation under air **as monitored by gravimetry (Figure**  
267 **6)**,

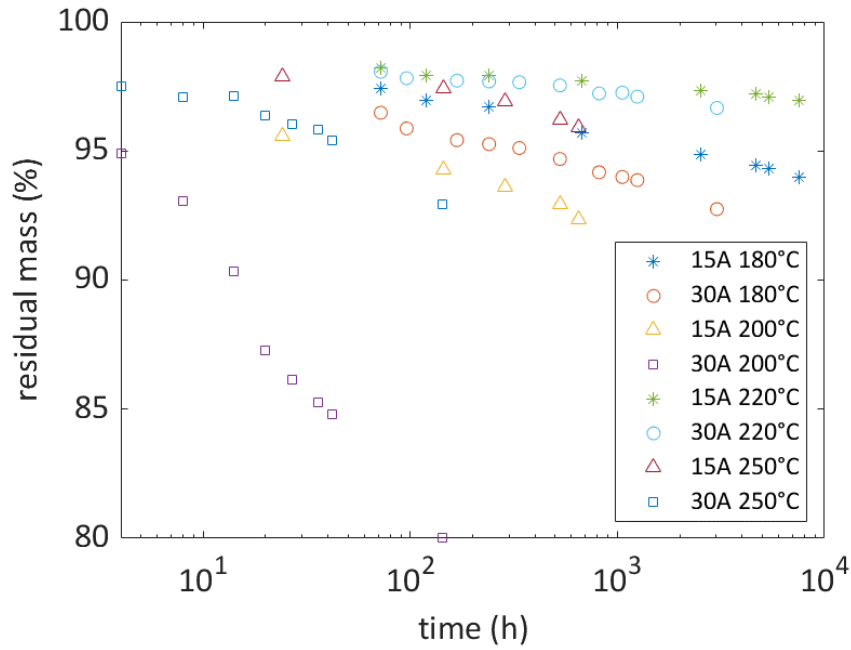
268 - in situ degradation in TGA cell of samples before and after thermal ageing (**Figure 7**).

269

270 According to **Figure 6**, PDMS aged under air showed a continuous mass loss. It means that  
271 despite a predominant crosslinking phenomenon **as seen above**, some chain scission phenomena  
272 occur and lead to the release of small volatile units **as already described in [1-3]**. It seems also  
273 that PDMS 30A is more stable **in terms of mass loss** than PDMS 15A. **According to our**  
274 **interpretation**, it suggests that crosslinking nodes exert a “stabilizing” effect regarding the  
275 mechanism responsible of mass loss.

276 This last result seems confirmed by TGA under the inert atmosphere (**Figure 7**). The  
277 comparison of virgin PDMS 15A and 30A highlights that crosslinking slows down the  
278 mechanisms responsible for mass loss. For each type of PDMS, the mass loss of the degraded  
279 samples was slower than the unaged material, suggesting that aging in air induces additional  
280 crosslinking.

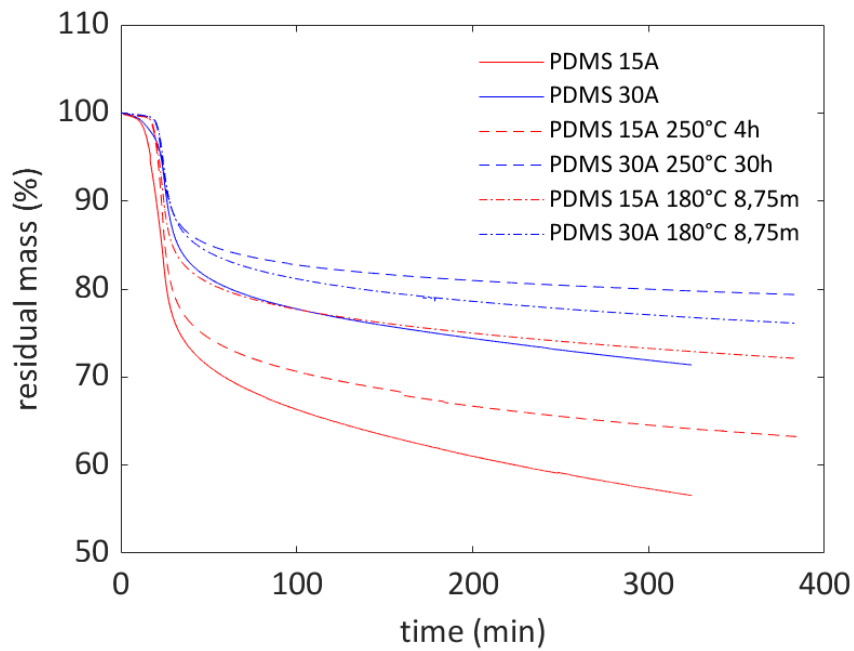
281



282

283

**Figure 6. Mass loss of PDMS aged under air.**



284

285

286

**Figure 7. TGA runs at 500°C under inert atmosphere for virgin and degraded PDMS samples.**

287

#### 288 4. DISCUSSION

289

290 The main purpose of this discussion section is to explain, describe and model the changes in  
 291 mechanical properties. To this end, possible mechanisms that occur at **molecular and**

23

24

292 **macromolecular scales** will be recalled together with their expected effects on mechanical  
 293 properties. In a second time, we will identify an adequate model for describing the hyperelastic  
 294 behavior of PDMS and its coefficient will be linked with macromolecular trackers describing  
 295 the occurrence of ageing. Finally, we will propose a possible embrittlement criterion for PDMS  
 296 under investigation.

297

#### 298 4.1. Degradation mechanism

299

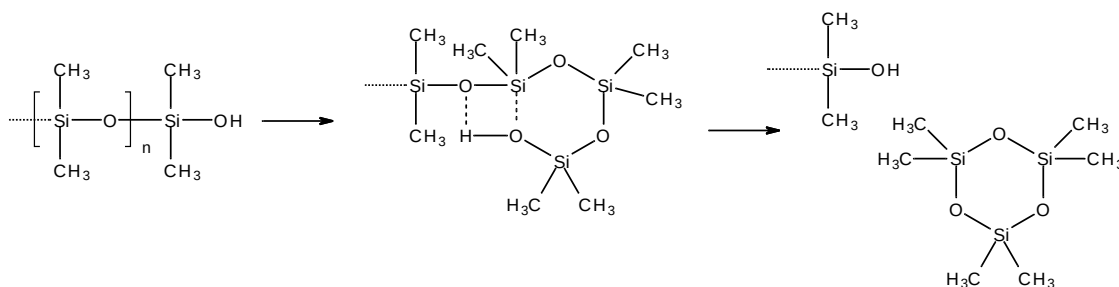
300 The main mechanisms **for thermal degradation** are described in the following.

301 **Under inert atmosphere**, several mechanisms are documented [1,2, 27, 28, 29]:

302 - end **initiated scission (Scheme 1a)**: this reaction decreases the size of the dangling chains,  
 303 **which do not participate to the elastic network** and might thus increase the crosslink density.

304 - random main chain scission (**Scheme 1b**): this reaction decreases the chain length between  
 305 crosslink. i.e. increase the crosslink density.

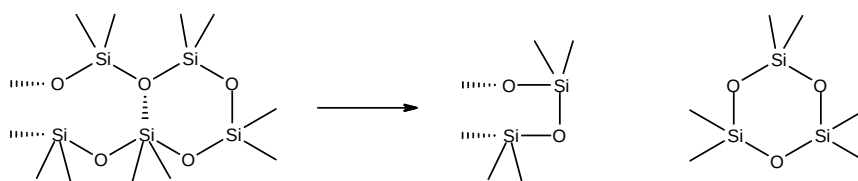
306 - externally catalyzed mechanisms for polymer containing impurities and residual catalyst.



307

308

(a)



309

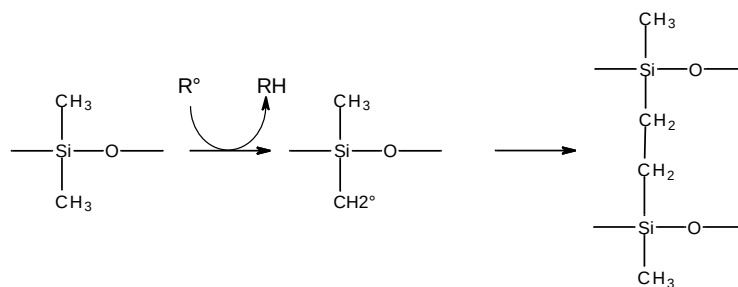
310

(b)

311 **Scheme 1. Unzipping mechanisms initiated by chain ends (a) and by random chain**  
 312 **scission (b) [24].**

313

314 **Under oxygen condition**, other reactions may occur. They involve the in-chain radical oxidation  
 315 of methyl groups as depicted in **Scheme 2**.



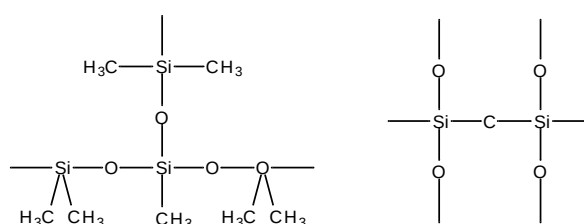
316

317

**Scheme 2. Possible mechanism of crosslinking [30].**

318

319 Some further mechanisms initiated by thermolysis of CH<sub>2</sub>-H, Si-O or Si-CH<sub>3</sub> may lead to the  
 320 formation of trifunctional nodes (**Figure 8**) [31].



321

322

**Figure 8. Nature of crosslink nodes formed by radical mechanisms [28].**

323 In any case, the balance of “thermolysis” mechanisms associated to unzipping and oxidation  
 324 processes, with two distinct activation energies explain that changes of mechanisms can be  
 325 observed with the ageing temperature. It is clear that the thermal aging mechanism may produce  
 326 some mass loss phenomena, but eventually lead to the observed increase in crosslink density.

327

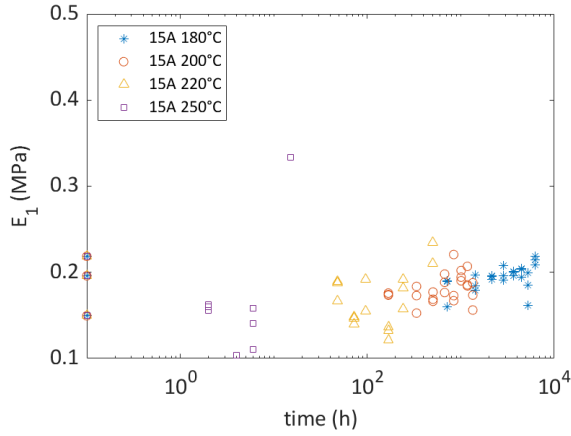
#### 328 4.2. Description of mechanical properties

329

330 There are two ways to describe the stress and strain curves and the changes during ageing time.  
 331 The first is based on the simple lecture of apparent elastic modulus at low and high deformation  
 332 [32]. A plot of modulus change versus time is given for several temperatures (**Figure 9**). An  
 333 increase was observed, which is evidence of the crosslinking process. **The increase of the**  
 334 **maximal value observed at the highest strains E<sub>2</sub> seems to be higher than observed at low strains**  
 335 **E<sub>1</sub>** consistently with previous reports showing a decrease of ultimate elongation and work to  
 336 break with minor change of hardness and modulus at 100% deformation for “naturally” aged  
 337 silicones rubbers [8]. The effect at high temperature is higher than at low temperature possibly  
 338 because a crossover of the various mechanism recalled in the last section. The case of PDMS  
 339 15A is interesting: **Figures 1-3** show the progressive embrittlement of the rubber family, but E<sub>1</sub>  
 340 and E<sub>2</sub> changes are hard to detect. In fact, the embrittlement is associated to the “faster” upturn  
 341 of stress and strain curves **i.e. the “high strain domain” occurs earlier, and the “low strain**  
 342 **domain” is progressively reduced and disappears**. This fact cannot be fully depicted by the  
 343 simple measurement of E<sub>1</sub> and E<sub>2</sub>, which led us to find other descriptors of PDMS ageing.

27

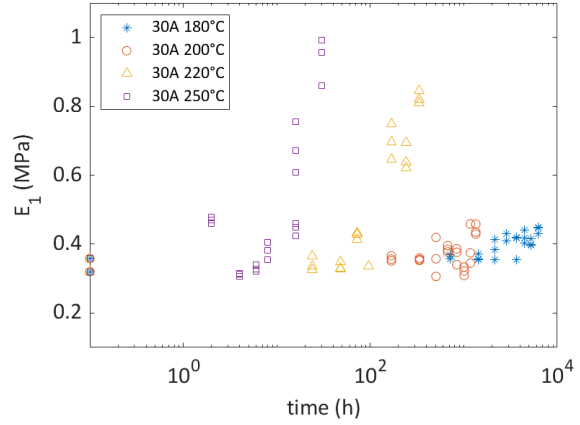
28



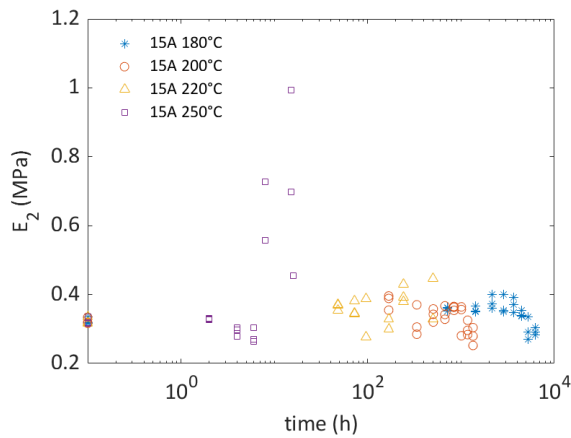
344

345

(a)



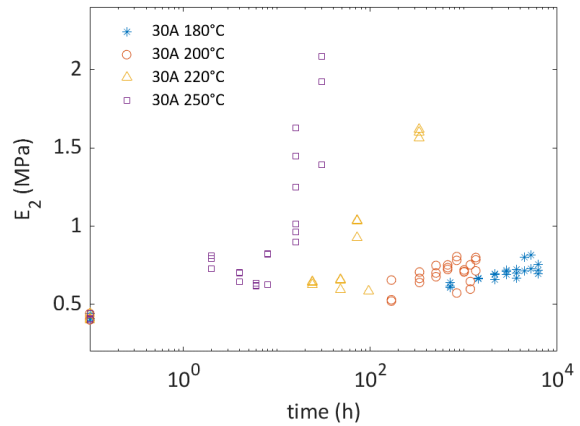
(b)



346

347

(c)



(d)

Figure 9. Changes of elastic moduli at low (a, b) and high strains (c, d).

348

349

350 Meanwhile  $E_1$  and  $E_2$  give a “local” description of the curve, the hyperelastic behaviour of virgin  
 351 and aged PDMS can also be represented through Mooney and Rivlin model [33] **at least for low**  
 352 **deformations** or the Ogden model [34] allowing the total description of the shape of the curve:

353

354

$$\sigma_0 = c_1 \cdot \left( \lambda^{\alpha_1 - 1} - \frac{1}{\lambda^{\frac{\alpha_1}{2} + 1}} \right) + c_2 \cdot \left( \lambda^{\alpha_2 - 1} - \frac{1}{\lambda^{\frac{\alpha_2}{2} + 1}} \right) + \dots \quad (6)$$

355

356 Formally, it is strictly equivalent to the Flory model of affine networks when  $c_2 = 0$  and  $\alpha_1 = 2$   
 357 [35]. In this last case,  $c_1$  directly expresses the entropic elasticity of Gaussian chains connected to  
 358 two crosslink nodes. Bernardi et al [14] have for example described the stress and strain curves  
 359 of unaged PDMS with an Ogden model made of three terms. Basing on [19], the hyperelastic  
 360 behavior will be justified as the sum of only two components: one given with  $\alpha_1 = 2$  **for long**  
 361 **elastic chains** and the second is characterized by an arbitrary fixed  $\alpha_2 = 3$  **parameter expressing**

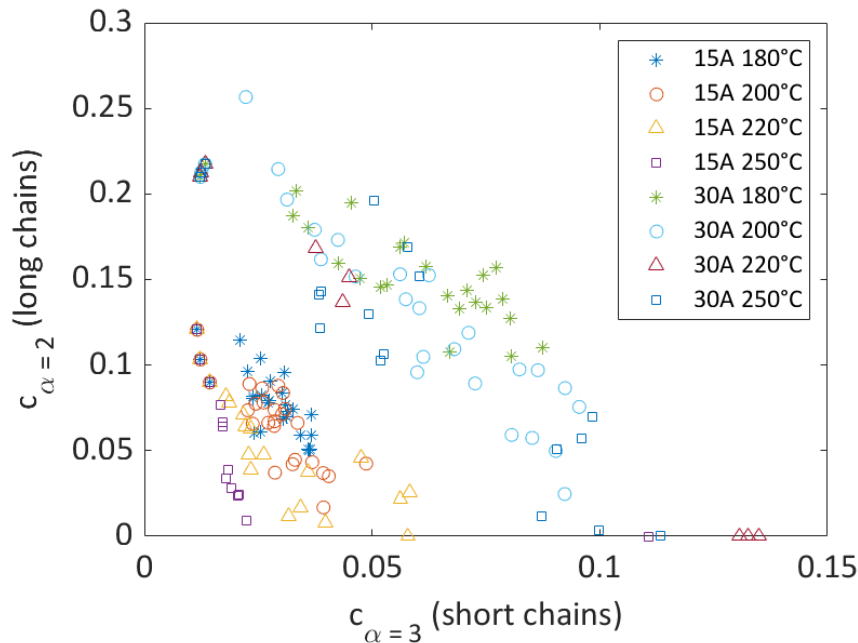
29

30



362 the presence of shorter chains. Its increase would express the occurrence of crosslinking process  
 363 as explained in the previous paragraph. In this approach,  $c_{\alpha=3}$  and  $c_{\alpha=2}$  represent the relative  
 364 contribution of each chain family. Those coefficients were extracted from a Matlab® routine  
 365 (see **Supplementary Information**). In general, very good fits ( $R^2 > 0.99$ ) were obtained (see  
 366 **Supplementary Information**).

367



368

369 **Figure 10. Changes of Ogden's coefficients for PDMS 15A and 30A aged at various**  
 370 **temperatures.**

371

372 The values are given in **Figure 10** calling for the following comments:

373 - overall, the contribution of « long » elastically active chains decreases because of the  
 374 appearance of « shorter » elastically active chains.

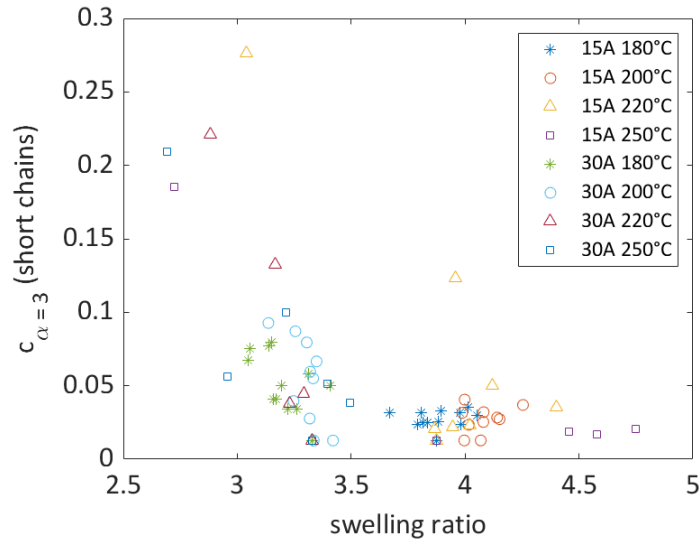
375 - interestingly, it seems that there is a slight effect of temperature: at higher temperatures e.g.  
 376 250°C, the ratio of short chains over long chains seems higher than at low temperatures e.g.  
 377 180°C. It means that the chemical mechanisms at the origin of the crosslinking are not exactly  
 378 the same, which can be discussed in terms of the relative contribution of reactions given in  
 379 **Schemes 1 and 2.**

380

381 Basing on **Figure 11**, the “physical” meaning of  $c_{\alpha=3}$  as an expression of the crosslinking  
 382 induced by thermal ageing can be tentatively justified: its increase results in a decrease of the  
 383 swelling degree, and in several parameters expressing the crystallization: onset temperature,  
 384 maximal crystallization temperature and crystallization enthalpy (see **Supplementary**  
 385 **Information**).

31

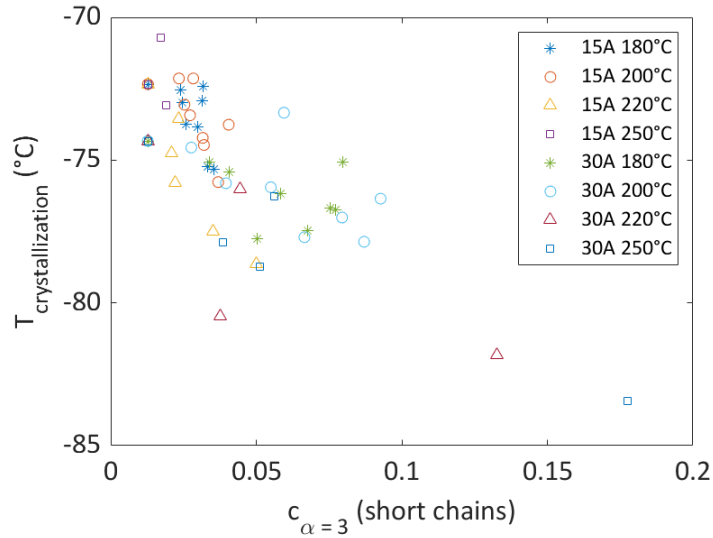
32



386

387

(a)



388

389

(b)

390 **Figure 11. Plot of swelling degree (a) and onset crystallization temperature (b) vs the**

391  **$c_{\alpha=3}$  component (see Eq. 6).**

392

393 **4.3. Proposal of an embrittlement criteria**

394

395 The last aim of this discussion is to link the changes of descriptors of the mechanical behavior  
 396 and in particular ultimate properties with Ogden **coefficients**. At first, it is noteworthy that  
 397 sample have lost most than 50% of their initial elongation at break whereas both swollen ratio  
 398 and mass loss display only very limited change (**Table 3**). Interestingly, mass loss is higher for  
 399 PDMS 15A samples than PDMS 30A, which is in line with results given in **Figure 7**.

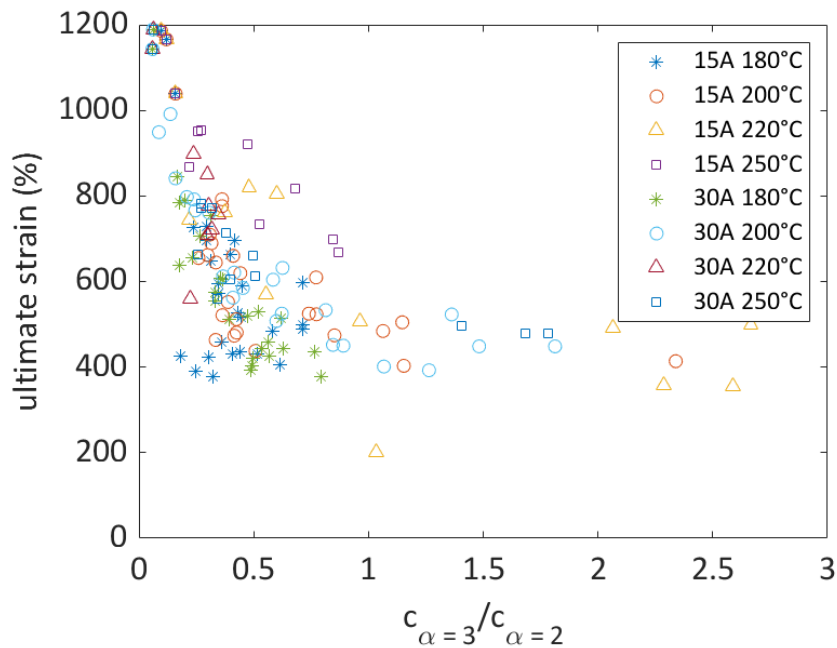
	15A				30A			
	$t_{50\%}$	SR	SF	mass loss	$t_{50\%}$	SR	SF	mass loss
<b>virgin</b>		3.9	0.21			3.3	0.05	
<b>250°C</b>	8 hours	2,7	0.13	6,50%	8 hours	3.2	0.08	3%
<b>220°C</b>	7 days	2,9	0.11	6%	3 days	3,2	0.07	3%
<b>200°C</b>	5 weeks	4.1	0.2	6%	5 weeks	3,3	0.07	3%
<b>180°C</b>	5 months	4	0.21	5%	5 months	3,3	0.07	3%

400 **Table 3. Changes of sol-gel properties and mass loss at “embrittlement” (here**  
 401 **corresponding to 50% of initial elongation at break).**

402

403 The **coefficients** can be proposed as another criterion for describing the stress and strain curves  
 404 **given in previous paragraph.**

405



406

407 **Figure 12. Changes of ultimate strain vs the ratio expressing the contribution of**  
 408 **short/long chains.**

409

410 Initially,  $c_{\alpha=3} \ll c_{\alpha=2}$  which corresponds to highly stretchable samples. Samples display an  
 411 ultimate strain lower than half its initial value when  $c_{\alpha=3} \sim c_{\alpha=2}$ . At this stage, it is noteworthy  
 412 that in general, swelling ratio stays close to its initial value, and mass loss level is moderate  
 413 **keeping in mind that a great part of mass loss occurs at early exposure time.**

35

36

414 Samples become fully brittle when  $c_{\alpha=3}/c_{\alpha=2}$  becomes much higher than 5 but at this degradation  
415 level, the determination of  $c_{\alpha=3}$  and  $c_{\alpha=2}$  by the Matlab® routine becomes quite unreliable.  
416 According to the sol gel measurements, it seems to correspond to a very lowered capability of  
417 network to swell into toluene, because of a higher crosslinking extent. It brings an explanation  
418 to the fact that both PDMS degrade almost at the same rate: PDMS 15A is initially less  
419 crosslinked than PDMS 30A. Mass loss (presumably of cyclic oligomers) is thus faster and  
420 leads to a faster increase of crosslink density.

421

## 422 5. CONCLUSIONS

423

424 This paper presents the thermal ageing at temperatures ranging from 180 to 250°C of two grades  
425 of Room Temperature Vulcanized silicone rubbers differing in the initially crosslinking  
426 densities. Ageing result in the depletion of ultimate elongation. The stress and strain curves  
427 remain almost unchanged in the low strain domain whereas the high strain domain displays the  
428 most significant changes: the apparent elastic modulus increases, and the « transition » between  
429 the « low » and « high » strain domains occurs earlier and earlier. Those results were interpreted  
430 by an overall crosslinking process due to the two possible chemical mechanisms: thermal  
431 unzipping and thermal oxidation.

432 In the ageing conditions under investigation, the ultimate properties are lost at « low »  
433 conversion degrees since sol-gel properties or mass loss display only slight changes. The  
434 concavity of the stress and strain curve **expressed by the coefficient of the Ogden model of**  
435 **hyperelastic solids** were used as an embrittlement criterion. It appears that sample became «  
436 brittle » when the contribution linked to short chains became higher than the contribution linked  
437 to long chains. It remains to pursue those investigations by a better understanding of the  
438 mobility and the relaxation of chains during the ageing process [<sup>36</sup>] and exploring the case of  
439 ageing modes leading to chain scissions **such as aminolysis** [<sup>37</sup>] for a better scrutiny of the  
440 proposed end of life criteria.

441

## 442 6. REFERENCES

---

37 <sup>1</sup> Camino G, Lomakin SM, Lazzari M (2001) Polydimethylsiloxane thermal degradation Part 1. Kinetic aspects.  
38 Polymer 42(6):2395-2402. [https://doi.org/10.1016/S0032-3861\(00\)00652-2](https://doi.org/10.1016/S0032-3861(00)00652-2)

39 <sup>2</sup>  
40 Camino G, Lomakin SM, Lagaard M (2002) Thermal polydimethylsiloxane degradation. Part 2. The degradation  
41 mechanisms. Polymer 43(7):2011-2015. [https://doi.org/10.1016/S0032-3861\(01\)00785-6](https://doi.org/10.1016/S0032-3861(01)00785-6)

42 <sup>3</sup>  
43 **N. Grassie, K.F. Francey. The thermal degradation of polysiloxanes—Part 3: Poly(dimethyl/methyl phenyl**  
44 **siloxane). Polymer Degradation and Stability 2(1), 1980, 53-66.**

45 <sup>4</sup>  
46 Lewicki JP, Worsley MA, Albo RLF, Finnie JA, Ashmore M, Mason HE, Baumann TF, Maxwell RS (2014) The effects  
47 of highly structured low density carbon nanotube networks on the thermal degradation behaviour of  
48 polysiloxanes. Polym Degrad Stab 102:25-32. <https://doi.org/10.1016/j.polymdegradstab.2014.02.013>

49 <sup>5</sup>

50

51

- 52 M. Englert, F. Minister, A. Moussaoui, W. Pisula. Mechanical properties of thermo-oxidative aged silicone  
53 rubber thermally stabilized by titanium oxide based fillers. *Polymer Testing* 115, 2022, 107726  
54 <sup>6</sup>
- 55 N.S. Tomer, F. Delor-Jestin, L. Frezet, J. Lacoste. Oxidation, Chain Scission and Cross-Linking Studies of  
56 Polysiloxanes upon Ageings. *Open Journal of Organic Polymer Materials* 2(2), 2012, 13-22  
57
- 58 <sup>7</sup> Gillen KT, Kudoh H (2020) Synergism of radiation and temperature in the degradation of a silicone elastomer.  
59 *Polym Degrad Stab* 181:109334. <https://doi.org/10.1016/j.polymdegradstab.2020.109334>  
60 <sup>8</sup>
- 61 D. Oldfield, T. Symes. Long term natural ageing of silicone elastomers. *Polymer Testing* 15(2), 1996, 115-128.  
62
- 63 <sup>9</sup> P. Banet, L. Chikh, T. Fouet, O. Fichet. Phenyl effect on properties evolution of silicone network under  
64 isothermal and dynamic high temperature aging. *Journal of Applied Polymer Science* 139, 2022, 52420.  
65
- 66 <sup>10</sup> D.W. Van Krevelen, K. Te Nijenhuis – Chap. 18. Properties Determining Mass Transfer In Polymeric Systems. In  
67 “Properties of Polymers – Their correlation with chemical structure; Their numerical estimation and estimation  
68 from additive group contribution. Fourth, completely revised edition 2009. Elsevier.  
69 <sup>11</sup>
- 70 Han R, Li Y, Zhu Q, Niu K (2022) Research on the preparation and thermal stability of silicone rubber composites:  
71 A review. *Comp C* 8:100249. <https://doi.org/10.1016/j.jcomc.2022.100249>  
72 <sup>12</sup>
- 73 Panou AI, Papadokostaki KG, Tarantili PA, Sanopoulou M (2013) Effect of hydrophilic inclusions on PDMS  
74 crosslinking reaction and its interrelation with mechanical and water sorption properties of cured films. *Eur Pol J*  
75 49(7):1803-1810. <https://doi.org/10.1016/j.eurpolymj.2013.04.004>  
76 <sup>13</sup>
- 77 Bernardi L, Hopf R, Sibilio D, Ferrari A, Ehret AE, Mazza E (2013) On the cyclic deformation behavior, fracture  
78 properties and cytotoxicity of silicone-based elastomers for biomedical applications. *Polym Test* 60:117-123.  
79 <https://doi.org/10.1016/j.polymertesting.2017.03.018>  
80 <sup>14</sup>
- 81 Bernardi L, Hopf R, Ferrari A, Ehret AE, Mazza E (2017) On the large strain deformation behavior of silicone-based  
82 elastomers for biomedical applications. *Polym Test* 58:189-198.  
83 <https://doi.org/10.1016/j.polymertesting.2016.12.029>  
84 <sup>15</sup>
- 85 Kong J, Tong Y, Sun J, Wei Y, Thitsartarn W, Jayven CCY, Kinyanjui Muiruri J, Wong SY, He C (2018) Electrically  
86 conductive PDMS-grafted CNTs-reinforced silicone elastomer. *Comp Sci Tech* 159:208-215.  
87 <https://doi.org/10.1016/j.compscitech.2018.02.018>  
88 <sup>16</sup>
- 89 Stricher AM, Rinaldi RG, Barrès C, Ganachaud F, Chazeau L (2015) How I met your elastomers: from network  
90 topology to mechanical behaviours of conventional silicone materials. *RSC Adv* 5:53713-53725.  
91 <https://doi.org/10.1039/C5RA06965C>  
92 <sup>17</sup>
- 93 Zhao J, Chen P, Lin Y, Chang J, Lu A, Chen W, Meng L, Wang D, Li L (2018) Stretch-Induced Crystallization and  
94 Phase Transitions of Poly(dimethylsiloxane) at Low Temperatures: An in Situ Synchrotron Radiation Wide-Angle  
95 X-ray Scattering Study. *Macromolecules* 51(21):8424-8434. <https://doi.org/10.1021/acs.macromol.8b01872>  
96 <sup>18</sup>
- 97 Le Gac PY, Broudin M, Roux G, Verdu J, Davies P, Fayolle B (2014). Role of strain induced crystallization and  
98 oxidative crosslinking in fracture properties of rubbers *Polymer* 55(10), 2535-2542.  
99 <https://doi.org/10.1016/j.polymer.2014.03.023>  
100 <sup>19</sup>
- 101 Llorente MA., Andrady AL, Mark JE (1981) Model networks of end-linked polydimethylsiloxane chains. XI. Use of  
102 very short network chains to improve ultimate properties. *J Polym Sci Polym Phys* 19(4):621-630.  
103 <https://doi.org/10.1002/pol.1981.180190406>  
104

---

106 <sup>20</sup>

107 Flory PJ, Rehner Jr J (1943). Statistical Mechanics of Cross-Linked Polymer Networks II. Swelling . J Chem Phys

108 11:521. <https://doi.org/10.1063/1.1723792>

109 <sup>21</sup>

110 Mark JE (1981). Rubber Elasticity. Journal of Chemical Education. 58(11):898-903

111 <https://doi.org/10.1021/ed058p898>

112 <sup>22</sup>

113 Chassé W, Lang M, Sommer JU, Saalwächter K (2012) Cross-Link Density Estimation of PDMS Networks with

114 Precise Consideration of Networks Defects. Macromolecules 45:899-912. <https://doi.org/10.1021/ma202030z>

115 <sup>23</sup>

116 Patel SK, Malone S, Cohen C, Gillmor JR, Colby RH (1992) Elastic Modulus and Equilibrium Swelling of

117 Poly(dimethylsiloxane) Networks. Macromolecules 25(20):5241-5251. <https://doi.org/10.1021/ma00046a021>

118 <sup>24</sup>

119 Rey T, Chagnon G, Le Cam JB, Favier D (2013) Influence of the temperature on the mechanical behaviour of filled

120 and unfilled silicone rubbers. Polym Test 32(3):492-501. <https://doi.org/10.1016/j.polymertesting.2013.01.008>

121 <sup>25</sup>

122 Labouriau A, Cady C, Gill J, Stull J, Ortiz-Acosta D, Henderson K, Hartung V, Quintana A, Celina M (2015) Gamma

123 irradiation and oxidative degradation of a silica-filled silicone elastomer. Polym Degrad Stab 116:62-74.

124 <https://doi.org/10.1016/j.polymdegradstab.2015.03.009>

125 <sup>26</sup>

126 Flory PJ (1955) Theory of crystallization in copolymers. Trans. Farad Soc 51:848-857.

127 <sup>27</sup>

128 Tasic A, Pergal MV, Antić M, Antic VV (2017) Synthesis, structure and thermogravimetric analysis of a,w-

129 telechelic polydimethylsiloxanes of low molecular weight. J Serb Chem Soc 82(12):1395-1416.

130 <https://doi.org/10.2298/JSC170427082T>

131 <sup>28</sup>

132 Lewicki JP, Liggit JJ, Patel M (2009) The thermal degradation behaviour of

133 polydimethylsiloxane/montmorillonite nanocomposites. Polym Degrad Stab 94(9):1548-1557.

134 <https://doi.org/10.1016/j.polymdegradstab.2009.04.030>

135 <sup>29</sup>

136 Thomas TH, Kendrick TC (1969) Thermal analysis of polydimethylsiloxanes. I. Thermal degradation in controlled

137 atmospheres. J Polym Sci A-2 Polym Phys 7(3):537-549. <https://doi.org/10.1002/pol.1969.160070308>

138 <sup>30</sup>

139 Tomer NS, Delor-Jestin F, Frezet L, Lacoste J (2012) Oxidation, Chain Scission and Cross-Linking Studies of

140 Polysiloxanes upon Ageings. Op J Org Polym Mat 2:13-22. DOI: 10.4236/ojopm.2012.22003

141 <sup>31</sup>

142 Hill DJT, Preston CML, Whittaker AK (2002) NMR study of the gamma radiolysis of poly(dimethyl siloxane) under

143 vacuum at 303 K. Polymer 43(4):1051-1059. [https://doi.org/10.1016/S0032-3861\(01\)00711-X](https://doi.org/10.1016/S0032-3861(01)00711-X)

144 <sup>32</sup>

145 Aguilar-Bolados H, Contreras-Cid A, Neira-Carrillo A, Lopez-Manchado M, Yazdani-Pedram M (2019) Removal of

146 Surfactant from Nanocomposites Films Based on Thermally Reduced Graphene Oxide and Natural Rubber. J

147 Comp Sci 3:31. <https://doi.org/10.3390/jcs3020031>

148 <sup>33</sup>

149 Rivlin RS (1948) Large elastic deformations of isotropic materials. II. Some uniqueness theorems for pure,

150 homogeneous deformation. Phil Trans Royal Soc London A 240 A:491-508.

151 <https://doi.org/10.1098/rsta.1948.0003>

152 <sup>34</sup>

153 Ogden RW (1972) Large deformation isotropic elasticity - on the correlation of theory and experiment for

154 incompressible rubberlike solids. Proc Roy Soc A 326:565-584. <https://doi.org/10.1098/rspa.1972.0026>

155 <sup>35</sup>

156 Flory PJ (1985) Molecular Theory of Rubber Elasticity. Polym J 17(1):1-12.

157 <sup>36</sup>

158

159

---

160 Somers AE, Bastow TJ, Burgar MI, Forsyth M, Hill AJ (2000) Quantifying rubber degradation using NMR. Polym  
161 Degrad Stab 70(1) :31-37. [https://doi.org/10.1016/S0141-3910\(00\)00076-8](https://doi.org/10.1016/S0141-3910(00)00076-8)  
162  
163 <sup>37</sup> Chang CL, Don TM, Shih-Jen Lee H, Sha YO (2004) Studies on the aminolysis of RTV silicone rubber and  
164 modifications of degradation products. Polym Degrad Stab 85:769-777.  
165 <https://doi.org/10.1016/j.polyimdegradstab.2003.12.001>